Comparing organic to inorganic photovoltaic cells: Theory, experiment, and simulation

Brian A. Gregg[a] and Mark C. Hanna
National Renewable Energy Laboratory, 1617 Cole Boulevard, Golden, Colorado 80401

(Received 23 July 2002; accepted 16 December 2002)

Charge carriers are photogenerated with very different spatial distributions in conventional inorganic photovoltaic (IPV) cells and in organic photovoltaic (OPV or excitonic) cells. This leads to a fundamental, and often overlooked, mechanistic difference between them. Carriers are generated primarily at the exciton-dissociating heterointerface in OPV cells, resulting in the production of electrons in one phase and holes in the other—the two carrier types are thus *already separated* across the interface upon photogeneration in OPV cells, giving rise to a powerful chemical potential energy gradient $\nabla \mu_{hv}$ that promotes the photovoltaic effect. This occurs also in high-surface-area OPV cells, although their description is more complex. In contrast, both carrier types are photogenerated together throughout the bulk in IPV cells: $\nabla \mu_{hv}$ then drives both electrons and holes in the same direction through the same phase; efficient carrier separation therefore *requires* a built-in equilibrium electrical potential energy difference $\varnothing_{\mathrm{bi}}$ across the cell. The open-circuit photovoltage V_{oc} is thus limited to $\varnothing_{\mathrm{bi}}$ in IPV cells, but it is often greater than $\varnothing_{\mathrm{bi}}$ in OPVs. The basic theory necessary to compare IPVs to OPVs is reviewed. Relevant experiments are described, and numerical simulations that compare semiconductor devices differing *only* in the spatial distribution of photogenerated carriers are presented to demonstrate this fundamental distinction between the photoconversion mechanisms of IPV and OPV devices. © *2003 American Institute of Physics.* [DOI: 10.1063/1.1544413]

INTRODUCTION

The conversion of solar energy into electrical or fuel energy is becoming ever more important as the environmental, political, and physiological costs of our current energy sources become more apparent. Solar cells made from inorganic semiconductors have been studied since the 1950s and have been used as renewable electric power sources in applications ranging from satellites to residential roof-tops since the 1960s.[1] Recently, several types of solar cells based on organic materials have appeared, raising the intriguing possibility of inexpensive solar cells that can be made on flexible substrates.[2–4] There are some well-known differences between the photoconversion mechanisms in inorganic photovoltaic (IPV) cells and in organic photovoltaic (OPV) cells; most obviously, that light absorption in OPV cells leads to the production of excitons (mobile excited states),[5,6] while in IPV cells it leads directly to the creation of free electron-hole pairs. This difference, however, has fundamental, and underappreciated, consequences for the theoretical description of the photoconversion process and for efforts to optimize the performance of OPV cells.

Here we review a simple and general theoretical treatment of photoconversion processes that is valid for conventional (IPV) cells as well as for all three currently existing types of OPV cells: dye-sensitized solar cells (DSSCs);[2] planar organic semiconductor cells;[3,7,8] and high-surface-area, or bulk-heterojunction cells.[4,9–12] This treatment may also be valid for quantum dot solar cells,[13] although we do not specifically consider them. The OPV cells may be based on organic dyes, semiconducting polymers, small semiconductor molecules, or on some combination of these species. In all cases, however, light absorption by the organic species results primarily in the production of excitons rather than free electron-hole pairs. To produce a substantial photovoltaic effect, the electrically neutral excitons must either be created at (DSSCs), or diffuse to, an interface where they dissociate into an electron in one phase and a hole in the other: thus, *the charge carriers are already separated upon photogeneration*.[14] Exciton dissociation also can occur at bulk trap sites, leading to one trapped carrier and one potentially free carrier, but this is often just a minor perturbation on the PV effect caused by interfacial exciton dissociation. Internal electric fields are usually not strong enough to cause exciton dissociation: Given typical values for the exciton radius $\sim$1 nm, and binding energy $\sim$0.25 eV,[6,15] a field of $>10^6$ V/cm would be required to cause excitons to dissociate.[16] We discuss the special features of the photoconversion process introduced by the interfacial excitonic carrier generation mechanism: Most importantly, the different factors limiting the achievable photovoltage in OPV cells relative to IPV cells.

We then employ a semiconductor device simulation program (SIMWINDOWS) to illustrate the significant differences in photovoltaic behavior resulting from the apparently minor difference in charge generation/separation mechanism that distinguishes conventional from excitonic solar cells. We compare the differences in charge-carrier distributions, recombination rates, and (photo) current density-voltage (J-V) curves of the two solar cell types while assuming identical

[a]Electronic mail: brian_gregg@nrel.gov

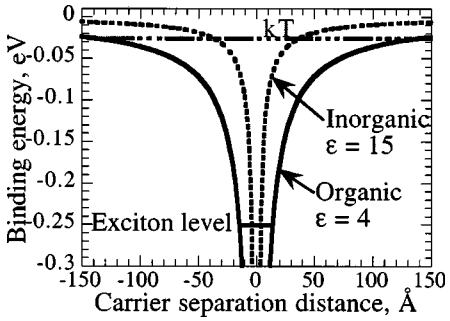

FIG. 1. Illustration of the binding energy between a photogenerated positive charge (hole) at the origin and a negative charge (electron) at the indicated distance from the hole. Potential wells were calculated for a typical inorganic semiconductor with an isotropic dielectric constant $\varepsilon = 15$ and a typical organic semiconductor ($\varepsilon = 4$) assuming point charges. The greater delocalization of the carrier wave functions (wider bandwidth, lower-effective mass), and the narrower Coulomb potential well in the IPV case, commonly result in the photoproduction of free electrons and holes at room temperature. In OPVs, however, localization of the carrier wave function (narrower bandwidth) and the wider Coulomb potential well lead to photoproduction of bound electron-hole pairs, or excitons.

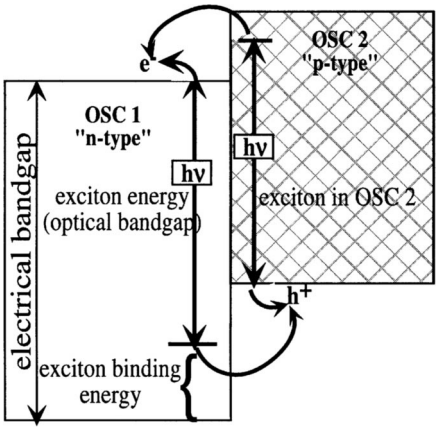

FIG. 2. Energy-level diagram for an excitonic solar cell with no band bending but a band offset. Excitons created by light absorption in both organic semiconductors 1 and 2 do not possess enough energy to dissociate in the bulk (except at trap sites). But the band offset between OSC1 and OSC2 provides an exothermic pathway for dissociation of excitons in both phases, producing electrons in OSC1 already separated from holes in OSC2. The band offset must be greater than the exciton binding energy for dissociation to occur.

band gaps, heterojunction band offsets, carrier mobilities, doping densities, thicknesses, etc. This provides a demonstration of the fundamental differences in photovoltaic behavior between IPV and OPV cells in otherwise identical devices.

Our discussion is at a general level: Although we may neglect some details of specific devices in favor of the ''big picture,'' we believe we have captured the essential mechanistic features that distinguish IPV from OPV devices. In the following, we always assume ohmic contacts for simplicity, that is, there is no voltage drop across the contacts, and the ratio of electrons to holes at the contacts always remains at its equilibrium value. We ignore small effects such as Dember potentials[1,6,17] and assume there are no temperature gradients (i.e., Seebeck effects are neglected).

EXCITONIC SOLAR CELLS

A key difference between organic (OPV) cells and conventional (IPV) solar cells (as epitomized by silicon *p-n* junction cells) is the relative importance of interfacial processes. This difference is closely related to the charge generation mechanism. Electron-hole pairs are generated immediately upon light absorption in IPV cells under normal conditions; that is, they are generated throughout the bulk according to the exponential decrease of the incident light intensity. In contrast, light absorption in organic materials almost always results in the production of a mobile excited state rather than a free electron-hole pair.[5,7,18] This occurs for two reasons (Fig. 1): (1) because the dielectric constant of the organic phase is usually low compared to inorganic semiconductors, the attractive Coulomb potential well around the incipient electron-hole pair extends over a greater volume than it does in inorganic semiconductors and (2) because the noncovalent electronic interactions between organic molecules are weak (narrow band width) compared to the strong interatomic electronic interactions of covalently bonded inorganic semiconductor materials like silicon, the electron's wave function is spatially restricted, allowing it to be localized in the potential well of its conjugate hole (and vice versa). Therefore, a tightly bound electron-hole pair (Frenkel exciton or mobile excited state) is the usual product of light absorption in organic semiconductors.[6] It is a mobile, electrically neutral species which, to first order, is unaffected by electric fields.

Electronic trap sites in the bulk can facilitate exciton dissociation into one trapped carrier and one free carrier, but this is not, in general, a viable mechanism for efficient photoconversion. However, it should be recognized that this process does occur to a greater or lesser degree in all OPV cells. The more fundamentally important process, and that which drives most OPV cells, is the interfacial dissociation of excitons at a heterointerface into a free electron in one material and a free hole on the other side of the interface (Fig. 2).[2,5,7,14,18–21] Except in DSSCs, excitons must first move, usually via diffusion[6,22] (and/or relaxation to lower-energy states in disordered materials), to the heterointerface and then dissociate (Fig. 2) by a mechanism that is not yet well understood.[6,16,22–24] The charge carriers are thus already separated from each other across the heterointerface upon generation. Given their usually low equilibrium carrier densities, excitonic solar cells under illumination are almost always majority carrier devices, unlike most IPV cells which are minority carrier devices. The energy of a thermalized exciton (which is the optical band gap) is less than the energy of a free electron-hole pair (electrical band gap); the difference being the exciton binding energy (Fig. 2). The thermodynamic requirements for interfacial exciton dissociation are clear—the band offset must be greater than the exciton binding energy (Fig. 2). But the kinetic requirements, and the role of interface polarizability, exciton transport rates, interfacial electronic states, etc., are not well understood. The crucial process of interfacial charge-carrier recombination is also poorly understood in solid-state OPV

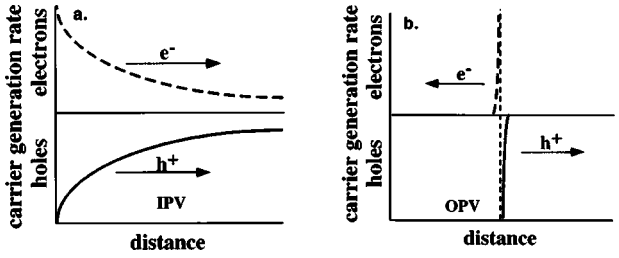

FIG. 3. A cartoon illustrating the difference in charge-carrier generation mechanisms in conventional (a) and excitonic (b) solar cells. In conventional solar cells (a), electrons and holes are photogenerated together wherever light is absorbed. Therefore, the photoinduced chemical-potential-energy gradient $\nabla\mu_{h\upsilon}$ (represented by arrows) drives both carrier types in the same direction. In the excitonic cell (b), however, electrons are photogenerated in one phase while holes are generated in the other via interfacial exciton dissociation. Carrier generation is simultaneous to, and identical with, carrier separation across the interface in OPV cells; $\nabla\mu_{h\upsilon}$ therefore drives electrons and holes in opposite directions.

cells,[25] although it is somewhat better characterized at the solid/liquid interface of DSSCs.[2,19,26–32]

Carrier generation and separation in IPV cells is also a multistep process, but the steps are different. Light absorption in IPV cells leads directly to the production of electron-hole pairs together in the same material. Since the two carrier types have the same spatial distribution in the same chemical phase, the photoinduced chemical potential energy gradient, $\nabla\mu_{h\upsilon}$ [Fig. 3(a)] drives them both in the same direction (although this is a small force in most IPVs). Therefore, electrons can be separated efficiently from holes in IPV cells *only* by the action of the electrical potential-energy gradient ∇U, more commonly known as the equilibrium electrical potential-energy difference across the cell, or band bending, $\varnothing_{\mathrm{bi}}$ ($=\int\nabla U(x)\,dx$ at equilibrium). In contrast to IPV cells, $\nabla\mu_{h\upsilon}$ in OPV cells drives both electron and holes *away* from the exciton dissociating interface [Fig. 3(b)], thus separating them further. This is also true, but complicated by geometrical factors, in the high-surface-area OPV cells discussed below. In most cases, $\nabla\mu_{h\upsilon}$ *complements* the effects of $\varnothing_{\mathrm{bi}}$ in OPV cells, while it *opposes* $\varnothing_{\mathrm{bi}}$ in IPV cells. This clearly leads to different limitations on the open circuit photovoltage V_{oc} for IPV and OPV cells.

It has become increasingly apparent that OPVs require a different description than IPVs. In 1990, we showed that a substantial PV effect could be achieved in an electrically symmetrical cell in which $\varnothing_{\mathrm{bi}}=0$.[18] A kinetic model based on the asymmetric dissociation of excitons at the porphyrin/ITO interface was developed to explain these results. Later, with the use of carrier-selective (energy-selective) contacts we achieved $V_{\mathrm{oc}}\sim 1$ V in OPV cells in which $\varnothing_{\mathrm{bi}}=0$.[33] More recently Malliaras *et al.* developed a kinetic model for polymer PV cells that included the spatially confined carrier generation profiles.[34] Brabec *et al.* showed that V_{oc} in polymer solar cells was not entirely controlled by $\varnothing_{\mathrm{bi}}$.[12] Then, Ramsdale *et al.* independently confirmed this result and explained it with a model that included the effect of the asymmetric interfacial dissociation of excitons.[35]

Carrier recombination is driven partly by the same forces that drive carrier separation and partly by kinetic factors that are still poorly understood.[25] Whether recombination occurs in the bulk [IPV cells, Fig. 3(a)] or at the exciton-dissociating interface [OPV cells, Fig. 3(b)] it is always an obstacle to efficient photoconversion.

INTERFACIAL CHEMICAL POTENTIAL GRADIENTS AND PHOTOVOLTAGE-DETERMINING MECHANISM

Conventional solar cells, almost by definition, all function according to the same photoconversion mechanism, one which is epitomized by silicon *p-n* junction solar cells. This mechanism is so well known that the assumptions underlying it are sometimes forgotten and it is thought to be the only possible mechanism for photoconversion. It has often been applied incorrectly to describe OPV cells. Here we review the generalized forces that drive a flux of electrons through a solar cell. This treatment does not make any device-specific assumptions, therefore it is valid for all types of solar cells.

The general kinetic expression for the one-dimensional current density of electrons $J_n(x)$ through any device is usually expressed as[1]

$$J_n(x)=n(x)\mu_n\nabla U(x)+kT\mu_n\nabla n(x), \tag{1}$$

where $n(x)$ is the concentration of electrons, μ_n is the electron mobility (not to be confused with the chemical potential energy μ), and k and T are Boltzmann's constant and the absolute temperature, respectively. An exactly analogous equation describes the flux of holes. The only assumption involved in this kinetic equation is that the electron current is affected only by electrical and chemical potential energy gradients; that is, that there are no magnetic fields, temperature or pressure gradients, etc. Equation (1) is valid both at equilibrium and away from it, both in the dark and in the light.

The quasi- (i.e., nonequilibrium) Fermi level for electrons in a semiconductor is defined as

$$E_{fn}(x)=E_{\mathrm{cb}}(x)+kT\ln\{n(x)/N_c\}, \tag{2}$$

where $E_{\mathrm{cb}}(x)$ is the electrical potential energy of the conduction-band edge, $E_{\mathrm{cb}}(x)=U(x)+\text{constant}$; and N_c is the density of electronic states at the bottom of the conduction band. Taking the gradient of Eq. (2) and substituting it into Eq. (1) provides the simplest expression for the electron current

$$J_n(x)=n(x)\mu_n\nabla E_{Fn}(x). \tag{3}$$

Thus, whenever $\nabla E_{Fn}\neq 0$, an electron current will flow through the device.

In the classical description of nonequilibrium systems, fluxes are driven by forces.[36] Equation (3) shows that the flux of electrons (J_n) is related to the (photo) electrochemical force (∇E_{Fn}) by a proportionality factor ($n\mu_n$). Equation (3) and the related equation for holes can be employed as a simple and powerful description of solar photoconversion systems. For example, *any* photoprocess that generates a nonzero value of ∇E_{Fn} and/or ∇E_{Fp} will result in a photovoltaic effect. This can be accomplished in a number of different ways, only one of which is employed in conventional *p-n* junctions. It is useful to break ∇E_{Fn} into its component quasithermodynamic constituents ∇U and $\nabla\mu$ to clearly re-

veal the difference between the photoconversion mechanisms of IPV and OPV cells. Equation (1) can be separated into two independent electron fluxes, each driven by one of the two nonequilibrium forces ∇U and $\nabla \mu$.

J_n due to the electrical potential energy gradient is

$$J_n(x) = n(x)\mu_n \times \nabla U(x). \tag{4a}$$

J_n due to the chemical potential energy gradient is

$$J_n(x) = n(x)\mu_n \times kT/n(x)\nabla n(x)$$

or

$$J_n(x) = n(x)\mu_n \times \nabla \mu(x). \tag{4b}$$

Again, these equations are equally valid in the light and in the dark. We employ $\nabla \mu_{hv}$ and ∇U_{hv} to denote these forces in a cell under illumination.

The expression for the chemical potential energy gradient

$$\nabla \mu(x) = kT/n(x)\nabla n(x) \tag{5}$$

can be derived by taking the spatial gradient of the equilibrium thermodynamic expression, $\mu = kT \ln(n) + \mu^0$.[37] Equations 4(a) and 4(b) show that the electrical potential energy gradient ∇U and the chemical potential energy gradient $\nabla \mu$ are *equivalent* forces. This equivalence is often overlooked because of the predominant importance of ∇U in IPV cells. In OPV cells, however, $\nabla \mu_{hv}$ is often the dominant force. Since almost all carriers are photogenerated at the interface in OPV cells, their concentration gradient (proportional to $\nabla \mu_{hv}$ and the carrier diffusion coefficient) is much higher than in IPV cells (with their spatially distributed carrier generation, Fig. 3). This effect, coupled to the spatial separation of the two carrier types across the interface upon photogeneration [Fig. 3(b)], constitutes a powerful photovoltaic driving force. Thus, ∇U can be ≈ 0, for example, and a highly efficient solar cell can be made based wholly on $\nabla \mu_{hv}$. This is how dye-sensitized solar cells (DSSCs) function,[19,32] in which the mobile electrolyte permeating the cell eliminates the internal electric fields (see below). In solid-state OPV cells without mobile electrolyte, both ∇U and $\nabla \mu$ must be taken into account.

It is possible to make solid-state OPV cells based entirely on $\nabla \mu_{hv}$, in which $\nabla U = 0$ at equilibrium (and we simulate the behavior of such cells below because of their theoretical simplicity). In this case, however, the electric field induced by interfacial charge separation ∇U_{hv} will oppose further charge separation. Nevertheless, substantial photovoltaic effects have been achieved in such OPV cells in which $\varnothing_{bi} = 0$.[18,20,33]

The maximum photovoltage obtainable in any solar cell at a given light intensity I can be derived from Eq. (3). Since ∇E_{Fn} and ∇E_{Fp} are the driving forces for the fluxes of electrons and holes, respectively, net current flow must stop when these gradients both become zero (ideal cells) or when the electron flux exactly cancels the hole flux (nonideal cells). The maximum possible photovoltage in any PV cell is thus given by the maximum splitting between the quasi-Fermi levels anywhere in the cell at open circuit.

$$qV_{oc,max}(I) = (E_{Fn} - E_{Fp})_{max}. \tag{6}$$

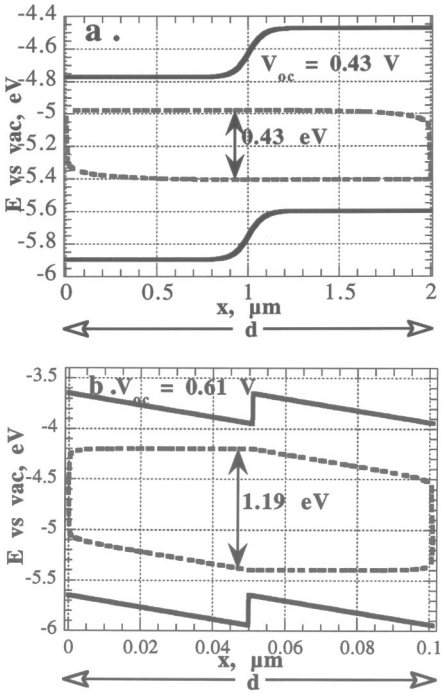

FIG. 4. (a) SimWindows simulation of a conventional silicon *p-n* junction solar cell at open circuit under 50 mW/cm^2 illumination at $\lambda = 2.5$ eV. The quasi-Fermi levels E_{fn} and E_{fp} are indicated as the upper- and lower-dashed lines, respectively. In this almost perfect IPV cell, $V_{oc}(I) = V_{oc,max}(I)$ because $\nabla E_{Fn} \approx 0$ on the *n*-type side and $\nabla E_{Fp} \approx 0$ on the *p*-type side. Therefore $E_{Fn,x=0} - E_{Fp,x=d} = (E_{Fn} - E_{Fp})_{max}$, see Eqs. (6) and (7). (b). A less-than-perfect OPV cell, in which there was no band bending at equilibrium (see Fig. 5), exhibits greater splitting of the quasi-Fermi levels under the same illumination because of its greater band gap, however $V_{oc}(I) < V_{oc,max}(I)$ because of substantial carrier recombination.

Any potential difference greater than this will cause the current to reverse direction. An example is shown in Fig. 4(a) for a simulated silicon *p-n* junction cell that exhibits almost perfect behavior in which $\nabla E_{Fn} \approx 0$ on the *n*-type side and $\nabla E_{Fp} \approx 0$ on the *p*-type side. Therefore, the ohmic electrodes charge up to the maximum possible potential difference for the given light intensity I. (The program used to calculate these results is described below).

The actual photovoltage in a solar cell, $V_{oc}(I)$, is usually less than $V_{oc,max}(I)$ because of recombination processes, mass transfer limitations, etc. [Fig. 4(b)]. Under the assumption of ohmic contacts

$$qV_{oc}(I) = E_{Fn,x=0} - E_{Fp,x=d}, \tag{7}$$

where $x = 0$ and $x = d$ correspond to the negative and positive contacts, respectively, of the solar cell (Fig. 4). An example of a solar cell exhibiting a less-than-maximum possible photovoltage is shown in Fig. 4(b). This is a special type of excitonic solar cell (see Fig. 5), designed for basic research rather than efficiency, in which there is no band bending at equilibrium except for the band offset ($\varnothing_{bi} = 0.3$ eV), and therefore ∇U_{hv} opposes $\nabla \mu_{hv}$.[18,20,33] In this case, $V_{oc}(I) < V_{oc,max}(I)$ because the quasi-Fermi levels decrease across the cell at open circuit due to recombination (see also Fig. 8 below). Equations (6) and (7) account for the

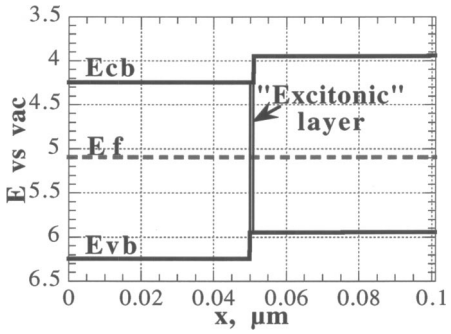

FIG. 5. An energy-level diagram, at equilibrium, of the simulated devices used to compare OPV to IPV cells. The only difference between them is that the OPV device absorbs light only in the ''excitonic'' layer, while the IPV device absorbs the same amount of light with a uniform absorption coefficient throughout the device. The contacts are assumed to be ohmic. Approximately 67% of the incident light is absorbed in the cell.

usual logarithmic increase of V_{oc} with light intensity through the logarithmic dependence of the quasi-Fermi levels on carrier concentrations [Eq. (2)].

In general, the photovoltage of a solar cell is a function of *both* electrical *and* chemical potential energy differences. The common assumption that $\varnothing_{bi}$ alone sets the absolute upper limit to the photovoltage (as $I \rightarrow \infty$)[5,17,38] is clearly not true in general. This assumption *is* true, however, for a specific photoconversion mechanism—namely, that which governs conventional solar cells. When both electrons and holes are photogenerated together in the same semiconductor phase, and thus have the same spatial distribution, $\nabla \mu_{hv}(x)$ drives them both in the same direction [Fig. 3(a)]. To separate electrons from holes then requires a built-in electric potential difference $\varnothing_{bi}$. In this case, $\varnothing_{bi}$ sets the absolute upper limit to V_{oc} *because* it is required for charge separation.

Excitonic solar cells, however, are fundamentally different: The charge-carrier pairs are already separated across an interface upon photogeneration creating a large $\nabla \mu_{hv}$ [Fig. 3(b)] which tends to separate them further; thus, an internal electric field is no longer a requirement for charge separation and $\varnothing_{bi}$ does *not* set the upper limit to V_{oc}. It has been shown experimentally in both solid state OPV cells[18,33] and in DSSCs[2,32] that $V_{oc} \approx 1$ V can be achieved under conditions where $\varnothing_{bi} \approx 0$. Numerical simulations of DSSCs also have shown that V_{oc} is practically independent of $\varnothing_{bi}$.[39] When experiments were designed to test the relative influence of $\varnothing_{bi}$ and $\nabla \mu_{hv}$ in OPV cells, $\nabla \mu_{hv}$ was shown to be capable of overwhelming $\varnothing_{bi}$.[20] Although perhaps counterintuitive when seen in the context of conventional solar cells, the fact that $q\ V_{oc}$ can be much greater than $\varnothing_{bi}$ could have been easily predicted on the basis of Eqs. 3–7.

$\nabla \mu$ plays a role in the current flow of all devices, but its importance declines as the equilibrium carrier concentration increases [Eq. (5)]. In metals, for example, the carrier concentration is so high that no significant concentration gradients can be achieved; therefore, the second term in Eq. (1) can be neglected. In highly doped semiconductors, significant values of $\nabla \mu$ can be achieved only in the minority carrier density. One reason for the importance of $\nabla \mu$ in OPV cells is the very low equilibrium charge density in most organic materials. Coupled to this, the interfacial charge generation process provides a strong driving force for charge separation. Of course, $\varnothing_{bi}$ still plays a role in most OPV cells. For photoconversion to be efficient, $\varnothing_{bi}$ must either promote current flow in the proper direction, as it does in most solid-state OPV cells,[3,4,12] or it must be neutralized, as it is in DSSCs.[2,32]

HIGH-SURFACE-AREA SOLAR CELLS

Both DSSCs and bulk heterojunction cells have a highly convoluted internal geometry that promotes charge generation and separation, but that also makes them more difficult to understand compared to devices with planar interfaces. The same physical principles that apply to planar junctions apply also to them, of course, but it becomes harder to visualize the forces when the interface is nanostructured in three dimensions. Since charge carriers are generated throughout the ''bulk'' in these OPV cells, albeit via interfacial exciton dissociation, it might be thought that they would behave more like an IPV cell than a planar excitonic cell. But this is incorrect. Since DSSCs are the more mature and better understood technology, we treat them first.

The presence of ~0.5 M mobile electrolyte ions permeating the entire nanostructured TiO_2 film in a DSSC eliminates all equilibrium or photoinduced electric fields with a screening length of ~1 nm.[2,40] Therefore, to a good approximation, the entire bulk of the device can be considered electric-field free, that is $\nabla U(x) = 0$. Furthermore, it has been shown both experimentally[19,32] and by numerical simulations[39] that changing the equilibrium electrical potential ($\varnothing_{bi}$) across the device via changes in the work functions of the electrodes has little or no effect on the device behavior. It was concluded that the PV effect in DSSCs is driven almost entirely by $\nabla \mu_{hv}$.[26,32,40]

Illumination leads to electron injection from the adsorbed dye into TiO_2 and hole injection into solution—again, the carriers are separated across the interface immediately upon photogeneration. This, by itself, means that V_{oc} is not solely determined by $\varnothing_{bi}$. But the spatial distribution of the photogenerated charge carriers in this case is essentially identical to that of the light absorption profile and thus $\nabla \mu_{hv}(x)$ will *initially* drive some electrons away from the substrate electrode (at $V < V_{oc}$). The *initial* values of $\nabla \mu_{hv}(x)$ upon illumination, however, are important only for transient measurements; it is the steady-state values of $\nabla \mu_{hv}(x)$ that determine the PV effect. At $V = V_{oc}$, the steady-state $\nabla \mu_{hv}(x)$ will be approximately zero throughout the TiO_2 as the interfacial recombination process balances the photoinjection and charge redistribution processes. The major potential drop occurs across the TiO_2/solution (electron conductor/hole conductor) interface. When producing power, that is, at $V < V_{oc}$, $\nabla \mu_{hv}$ drives electrons toward the substrate electrode. The flux of holes to the counter electrode occurs by a similar mechanism. Therefore, even though the photogenerated carrier profile is similar to that in an IPV cell, the fact that carriers are already separated from each other across the interface upon generation, and the fact that

bulk electric fields are eliminated, leads to a powerful PV effect driven almost entirely by $\nabla\mu_{hv}$.[19] It is worth noting that the DSSC is still by far the most efficient of the OPV cells.

Bulk heterojunction cells have a nanostructured morphology similar to DSSCs but lack mobile electrolyte. Therefore, electric fields must be taken into account. In the most efficient cells to date, an electron conducting, nanoparticulate phase (e.g., derivatized C_{60}^4 or CdTe quantum rods[11]) is dispersed at a concentration substantially above its percolation threshold into a hole-conducting polymer phase. Excitons generated in either phase dissociate at the nanostructured interface. Electrical contacts are made from two materials with different work functions, e.g., ITO and Al, and the associated built-in field helps drive electrons to the Al contact and holes to the ITO contact. As in DSSCs,[19,26] it is primarily by virtue of the extremely large asymmetry between the rapid interfacial exciton dissociation rate and the very slow interfacial recombination rate[41] that a substantial PV effect is achieved. Although much remains to be learned about bulk heterojunction cells, it is safe to say that $\nabla\mu_{hv}$ plays a role in them very similar to its role in DSSCs, but modified by the presence of both bulk and nanoscopic electric fields. Therefore, V_{oc} in bulk heterojunction cells is a function of both $\varnothing_{bi}$ and $\nabla\mu_{hv}$, as well as being strongly dependent on the interfacial recombination rate.

SIMULATIONS

Some of the experimental and theoretical factors that distinguish IPV from OPV cells were described above. The most fundamental difference between them is quite simple, involving just the spatial distribution of the photogenerated charge carriers. Therefore, it should be possible to reproduce much of this difference in behavior between IPV and OPV cells with a semiconductor device simulation program. To test this proposition, we employed the freeware simulation program SIMWINDOWS (http://www-ocs.colorado.edu/SimWindows/simwin.html).[42,43] This program is designed to simulate the behavior of conventional semiconductor devices such as solar cells, vertical cavity lasers, light-emitting diodes, etc. It numerically solves the coupled differential equations (transport, continuity, and Poisson's) that describe optoelectronic phenomena in semiconductor devices. By design, it equates light absorption with charge-carrier generation. SIMWINDOWS is thus ideally suited to describe IPV devices; but in order to employ it to compare IPV to OPV cells, we needed to adapt it to simulate the interfacial exciton dissociation process. Hence, we made the following assumption for the simulated OPV cells: Light absorption occurred only in a 1 nm thick ''excitonic'' interfacial film at the heterojunction between the two organic semiconductors. (To our knowledge, no *homojunction* OPV cells have been reported, probably due to the difficulty of doping organic semiconductors.[44]) This ''excitonic'' layer was designed to mimic as closely as possible the excitonic charge generation process: We set the conduction-band edge at the potential of the more negative semiconductor and the valence-band edge at the potential of the more positive semiconductor (Fig. 5). Excitations in this excitonic layer thus naturally lead to electron transfer to the left, and hole transfer to the right in Fig. 5, as well as to recombination in the excitonic layer.

To make the cleanest comparison with the OPV cell, this excitonic layer was also included in the IPV device. But in the IPV case, the light absorption coefficient was set constant throughout the cell. An energy-level diagram of the simulated devices is shown in Fig. 5. When illuminated, the light is incident on the left-hand side (lhs). The doping levels were set such that the bands in both the ''*n*-type'' (lhs) and ''*p*-type'' (rhs) layer are flat at equilibrium to simplify the comparison; both semiconductors have the same band gap (2.0 eV) and thus the band offset barrier for electrons (0.3 eV) is the same as that for holes. All carrier mobilities are set to 1 $cm^2/V\,s$. The only difference between the IPV and OPV cells in our comparison is that the absorption coefficient is $\alpha = 10^5\ cm^{-1}$ everywhere throughout the 101 nm thick IPV cell, while $\alpha = 10^7\ cm^{-1}$ in the 1 nm thick ''excitonic layer'' of the OPV cell and $\alpha = 0\ cm^{-1}$ elsewhere. The amount of light absorbed is thus practically the same in both cells; only its spatial distribution, and therefore the spatial distribution of photogenerated charge carriers, differ between the simulated OPV and IPV cells. We emphasize that the simulations are not meant to correspond quantitatively to any actual solar cells.

This is a reasonable, but still imperfect, model for excitonic (OPV) solar cells. It neglects light absorption in the bulk and exciton diffusion to the interface—the rate of light absorption in the excitonic layer in the model is thus equivalent to the rate of excitons arriving *and* dissociating at the interface in a real OPV cell. So the important problems of exciton diffusion and dissociation kinetics[22,24] are not addressed here. Light absorption in the OPV model produces only electrons in one OSC and only holes in the other, except for the few minority carriers that are thermally emitted over the band offset barrier. So far, this is a realistic representation of an excitonic cell. However, the existence of high concentrations of *both* electrons and holes together in the 1 nm thick ''excitonic'' layer of the model is not physical. In a true excitonic cell, there is no ''excitonic layer:'' Electrons are simply injected into one OSC and holes into the other by interfacial exciton dissociation. Essentially all recombination is interfacial in a real OPV cell, while in the model it occurs almost entirely in the excitonic layer by the same mechanisms (primarily Schockley–Hall–Read recombination) that occur in bulk semiconductors. There is as yet very little known about the interfacial recombination mechanism(s) in OPV cells, so the assumption of bulklike recombination in the excitonic layer seems, for the moment, as reasonable as any other assumption.

The simulated photocurrent-voltage curves for the two different types of cells under ~1 sun illumination are shown in Fig. 6. The IPV cell generates a weak PV effect. The photovoltage, $V_{oc} \approx 0.3$ V, is determined by the band offset at the heterointerface, $\varnothing_{bi} = 0.3$ eV, because the band offset rectifies the photocurrent: Electrons diffusing to the left and holes diffusing to the right will ''fall'' over the barrier and tend not to return. Thus, as usual in conventional cells, V_{oc} is limited to $\varnothing_{bi}$. Under applied bias, the current can have

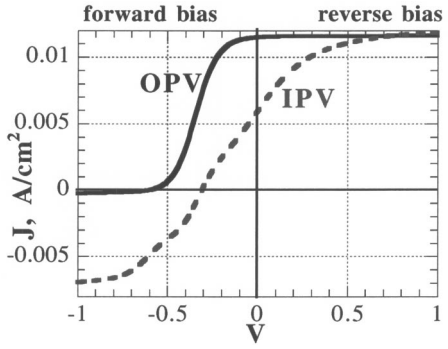

FIG. 6. The simulated photocurrent density-voltage curves for the two cells described in Fig. 5. Illumination as in Fig. 4.

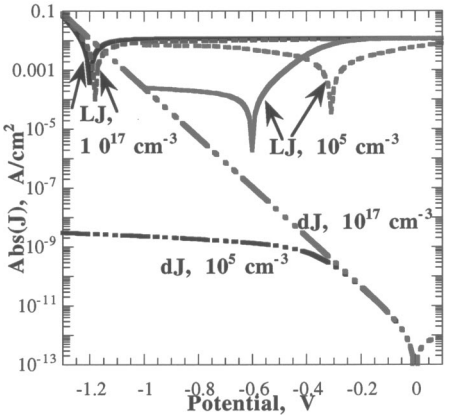

FIG. 7. Simulated dark currents, dJs, and photocurrents, LJs, as a function of doping levels in cells like that shown in Fig. 5. The dJs, dot-dashed lines, are identical for both IPV and OPV cells. The solid and dashed lines represent the LJs of the OPV and IPV cells, respectively. 10^5 cm^{-3} means the doping density on the lhs is $N_d = 10^5$ cm^{-3} and on the rhs, $N_a = 10^5$ cm^{-3}. The doping level of 10^{17} cm^{-3} corresponds to $\varnothing_{bi} = 1.7$ eV. Illumination as in Fig. 4. The data for LJ, 10^5 cm^{-3} are from Fig. 6.

either positive or negative polarity in the IPV device because both carrier types are photogenerated throughout the bulk. The applied potential can then drive photogenerated carriers in either direction, although it is more efficient to drive them in the ''downhill'' direction relative to the band offsets (Fig. 6).

The OPV cell generates a much stronger PV effect (Fig. 6) than the IPV cell because the charge carriers are generated only at the heterointerface and they are already separated across the phase boundary. This produces a large chemical potential gradient [Fig. 3, Eqs. (1) and 4(b)], in addition to the rectifying effect of the band offset, that drives the electrons toward the negative electrode and the holes toward the positive electrode. This beneficial force due to $\nabla \mu_{hv}$, is lacking in the IPV cell. Therefore, J_{sc} and the fill factor are higher than in the IPV case, and $V_{oc} = 0.6$ V in a cell in which $\varnothing_{bi} = 0.3$ eV. Figure 4(b) shows the band diagram of the same cell at open circuit. This simulation, and a number of other experimental and simulated results,[2,12,18–20,32,35,39,45] show that there is nothing unusual about obtaining $q V_{oc} > \varnothing_{bi}$. In fact, this is often expected for an OPV cell because the PV effect is *enhanced* by the interfacial $\nabla \mu_{hv}$.

Under ''forward'' bias, the OPV cell shows only a very small current (Fig. 6). This is a consequence of the low-doping density (1.4×10^5 cm^{-3}) and of electrons being photogenerated only on the lhs of the device (Fig. 5) and holes only on the rhs. When the applied bias drives the photogenerated carriers back toward the interface (forward bias for a *p-n* junction), they can only recombine (their usual fate) or be thermally emitted over the heterointerface barrier. The very low current in the ''forward'' bias direction is due to thermal emission over the interfacial barrier (the effective width of which is potential dependent). We have observed such behavior experimentally in OPV cells (not shown). This is in contrast to the IPV device in which photogenerated electrons on the rhs and holes on the lhs produce a substantial current under forward bias.

In many actual devices, the very low-''forward'' bias current (Fig. 6) that is diagnostic of a low-doped excitonic solar cell is obscured. For example, if the exciton-dissociating interface does not cleanly rectify the current (e.g., the doped SnO_2/liquid crystal porphyrin interface[18]) there can be a substantial current under ''forward'' bias because either electrons or holes, depending on applied potential, can be injected across the interface. It may also be obscured by the dissociation of photogenerated excitons at trap states in the bulk. This leads to the production of one free carrier and one trapped carrier in the bulk, resulting in photoconductivity (sometimes misleadingly referred to as ''photodoping''). Finally, facile carrier injection from the electrodes (observable as a dark current) can also obscure the characteristic *J-V* behavior of an excitonic solar cell.

The simulated dark currents for both the IPV and OPV cells of Fig. 5 were identical and were many orders of magnitude lower than the photocurrents (Fig. 7). The very low-dark current is a result of the low doping, the ohmic contacts and the lack of intragap states. Therefore, only carriers thermally emitted from the ohmic contact into either the conduction- or valence-bands contribute substantially to the dark current, because the equilibrium carrier concentration in these almost intrinsic semiconductors is insignificant.[5–7] In such cells, IPV or OPV, one cannot quantitatively compare dark currents to photocurrents,[7] as is commonly done in conventional, highly doped PV cells. The number of photogenerated carriers constitutes such a major perturbation on the equilibrium carrier density that the photocurrents are qualitatively different from the dark currents.[26]

The changes in the simulated *J-V* behavior with doping density were investigated. In the cells shown in Figs. 4(b), 5, and 6, the doping density was set such that there was no band bending at equilibrium (except for $\varnothing_{bi} = 0.3$ eV at the heterointerface) in order to eliminate one of the two driving forces for electron transfer through the bulk. The resulting doping densities ($N_a = N_d = 1.4 \times 10^5$ cm^{-3}), although far higher than the intrinsic carrier levels for semiconductors of band gap $= 2.0$ eV, are still lower than what is generally measured for molecular semiconductors.[5] It is quite difficult to dope molecular semiconductors[44,46] and most of what appear to be dopants in OSCs are probably either electron or hole traps.[6] Nevertheless, we simulated a series of cells like those shown in Fig. 5 but with doping densities ranging from 10^5 to 10^{17} cm^{-3}, corresponding to $\varnothing_{bi}$ ranging from 0.3 (the band

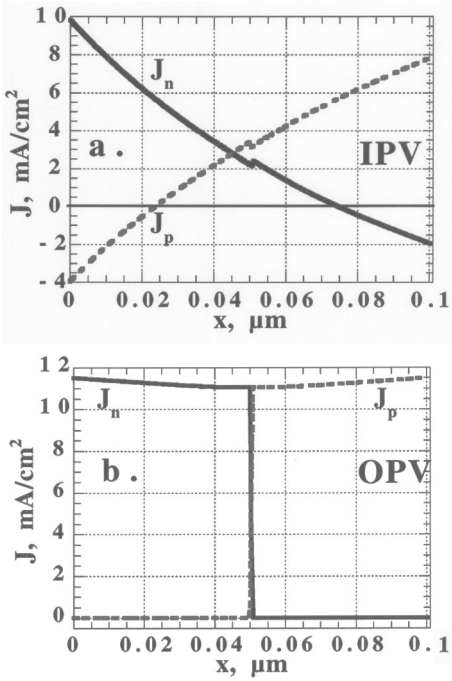

FIG. 8. The simulated electron photocurrent (J_n, solid line) and the hole photocurrent (J_p, dashed line) for both (a) IPV and (b) OPV cells under illumination at short circuit. The simulated cells are those of Figs. 4(b), (5), and (6); illumination as in Fig. 4.

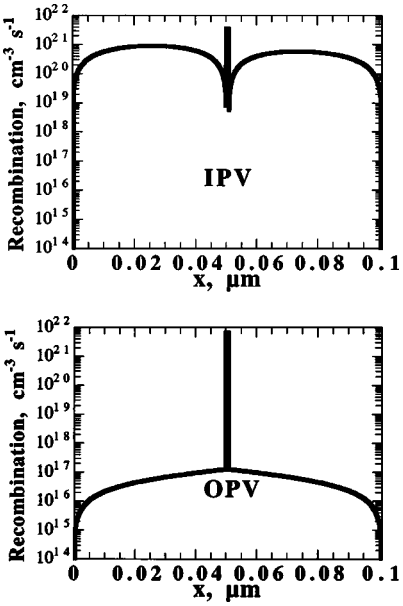

FIG. 9. Simulated recombination rates vs distance at short circuit. Recombination occurs primarily in the bulk in the IPV cell, and predominantly at the interface in the OPV cell.

offset level) to 1.7 eV. The doping density of the *n*-type side was always set equal to that of the *p*-type side, that is, $N_d = N_a$. Only the *J-V* curves of the lowest- and highest-doping densities are shown in Fig. 7; all others ranged uniformly between the two shown. The dark currents were identical for the OPV and IPV devices, of course, since the only distinction between them is the spatial distribution of *photo*generated carriers. The dark currents under forward bias increased steadily with doping density, and the transition between the region of exponentially increasing dark current and the linear region of resistance-limited current moved steadily to more negative potentials. The photo *J-V* curves at the lowest doping density in Fig. 7 also were shown in a linear graph in Fig. 6. The corresponding curves at the highest-doping density show the same limiting photocurrent as at low-doping density, but much higher V_{oc} and fill factor caused by the greatly increased driving force for carrier separation. Still, the OPV cell has a higher-fill factor and a slightly higher V_{oc} than the IPV cell, showing that two driving forces for charge separation (∇U plus $\nabla \mu$) are better than just one (∇U), all else being equal. Only when the doping density approached 10^{17} cm^{-3} did the photocurrents start to quantitatively match the dark currents, offset by J_{sc}, as expected for a conventional IPV cell. From now on, the results and discussion refer again exclusively to the low-doped devices in which the bands are flat everywhere except at the heterointerface.

Figure 8(a) shows the individual carrier currents in the illuminated IPV cell of Fig. 5 at short circuit. This quantity is directly proportional to the gradient of the carrier concentrations in a cell with no electric field [see Eq. (1)]. There are higher currents of electrons on the lhs and holes on the rhs because the band offsets effectively prevent diffusion of electrons to the right, and holes to the left across the heterointerface. The total photocurrent density through the cell $J_{tot}=J_n+J_p$ is much less than it could be because holes are photogenerated on the ''*n*-type'' side (lhs) and electrons on the ''*p*-type'' side (rhs) leading to substantial recombination. The electron flux to the lhs electrode at short circuit is only ~2.5 fold higher than the flux of holes. In other words, ~40% of the possible photocurrent is lost because both electrons and holes are flowing to the same electrode where they recombine.

In contrast, Fig. 8(b) shows that the interfacial photogeneration process in the OPV cell results in a very high degree of rectification of the photocurrent: The electron flux to the illuminated electrode is $>10^5$ times higher than the hole flux. This is because only electrons are injected into the lhs phase via exciton dissociation, and the only holes present in this phase are those resulting from thermal emission over the 300 meV potential-energy barrier at the heterointerface. Thus, recombination in the bulk and at the electrical contacts in these majority carrier devices is insignificant; the only significant recombination occurs at the exciton dissociating interface.

Recombination of photogenerated charge carriers is the bane of all solar cells, and it is usually what prevents them from reaching their theoretical efficiency limits. The spatial variation of the recombination rates of the two types of simulated solar cells are shown in Fig. 9. As expected from the charge generation mechanisms, recombination in the IPV cell occurs mainly in the bulk, while recombination in the OPV cell occurs mainly at the interface. Minimizing the recombination rate is one of the most important endeavors in the development of any solar cell, and it is clear that very different procedures are required for IPV and OPV cells. Bulk properties are most important for IPV cells because

carriers are photogenerated and also recombine in the bulk. Interface properties are most important in OPV cells because carriers are photogenerated and recombine at the interface. Optimizing bulk properties, such as crystallinity, is therefore key to the performance of IPV cells; while optimizing interfacial properties, such as maximizing the exciton dissociation rate and minimizing the interfacial recombination rates,[22,26] are essential for improving OPV cells.

These simulations prove that a simple difference in the spatial location of photogenerated charge carriers, with every other parameter held constant, results in fundamental changes in photovoltaic behavior. This simple difference in mechanism is exactly that which most fundamentally distinguishes IPV cells from OPV cells, as also described above by theory and by comparison to a multitude of experimental results.

SUMMARY AND CONCLUSIONS

The photoinduced generation of a free electron and hole in OPV cells is simultaneous with, and identical to, the initial separation of the electron from the hole across the interface. This is a fundamental mechanistic difference relative to conventional solar cells, in which generation and separation are two spatially and temporally distinct processes (Figs. 2 and 3). This results in different limiting factors for the photovoltages of the two cell types. Conventional solar cells *require* a gradient of electrical potential to separate the photogenerated charge carriers efficiently. Thus, the built-in electrical potential-energy difference at equilibrium, $\varnothing_{\mathrm{bi}}$, sets an upper limit to the achievable photovoltage. In OPV cells, on the other hand, the two carrier types are already separated across a phase boundary upon photogeneration. In this case, $\varnothing_{\mathrm{bi}}$ by itself does not limit the photovoltage in an OPV cell; rather V_{oc} is also influenced by, or even controlled by, the photoinduced chemical-potential difference across the interface $\Delta\mu_{hv}$.

The importance of $\nabla\mu_{hv}$ in OPVs derives from several factors: (1) The interfacial exciton dissociation process that results in a high concentration of photogenerated electrons on one side of the heterointerface and holes on the other; (2) the slow interfacial recombination process that allows the buildup of a substantial concentration of each charge carrier in its respective phase; and (3) the low concentration of equilibrium carriers that accentuates the effect of the photogenerated carrier concentration.

In many articles that have discussed V_{oc} in OPV cells, the assumption is made either explicitly or implicitly that $q\,V_{\mathrm{oc,max}}=\varnothing_{\mathrm{bi}}$. The authors are then forced to explain the often anomalously large values of V_{oc} by various mechanistic and/or thermodynamic contortions. But these problems are caused entirely by the erroneous assumption that $q\,V_{\mathrm{oc,max}}=\varnothing_{\mathrm{bi}}$. Although this holds true for conventional IPV cells, it is almost never true for OPV cells. We are aware of no case in which the published data on OPV cells cannot be explained by the simple and logically unimpeachable assumption that the photovoltage is determined by *both* $\nabla\mu_{hv}$ and $\varnothing_{\mathrm{bi}}$. This is expected theoretically for all solar cells. It may be overlooked in IPV cells because they function by a mechanism that emphasizes the importance of $\varnothing_{\mathrm{bi}}$, but in OPV cells, $\Delta\mu_{hv}$ often plays the predominant role because charge carriers are photogenerated via the interfacial exciton dissociation process. This, we believe, is the most important mechanistic difference between IPV and OPV cells, and it must be taken into account in order to understand the OPV cells and to optimize their efficiencies.

The device files and parameter files used in the simulations are available as supplemental material.[47]

ACKNOWLEDGMENT

We thank the U.S. DOE, Office of Science, Division of Basic Energy Sciences, Chemical Sciences Division, for supporting this research.

[1] A. L. Fahrenbruch and R. H. Bube, *Fundamentals of Solar Cells. Photovoltaic Solar Energy Conversion* (Academic, New York, 1983).
[2] A. Hagfeldt and M. Grätzel, Acc. Chem. Res. **33**, 269 (2000).
[3] P. Peumans, V. Bulovic, and S. R. Forrest, Appl. Phys. Lett. **76**, 2650 (2000).
[4] S. E. Shaheen, C. J. Brabec, N. S. Sariciftci, F. Padinger, and T. Fromherz, Appl. Phys. Lett. **78**, 841–843 (2001).
[5] J. Simon and J.-J. Andre, *Molecular Semiconductors* (Springer-Verlag, Berlin, 1985).
[6] M. Pope and C. E. Swenberg, *Electronic Processes in Organic Crystals and Polymers*, 2nd ed. (Oxford University Press, New York, 1999).
[7] B. A. Gregg, Chem. Phys. Lett. **258**, 376 (1996).
[8] S. A. Jenekhe and S. Yi, Appl. Phys. Lett. **77**, 2635 (2000).
[9] J. J. M. Halls, C. A. Walsh, N. C. Greenham, E. A. Marseglia, R. H. Friend, S. C. Moratti, and A. B. Holmes, Nature (London) **376**, 498 (1995).
[10] G. Yu, J. Gao, J. C. Hummelen, F. Wudl, and A. J. Heeger, Science **270**, 1789 (1995).
[11] W. U. Huynh, J. J. Dittmer, and A. P. Alivisatos, Science **295**, 2425 (2002).
[12] C. J. Brabec, A. Cravino, D. Meissner, N. S. Sariciftci, T. Fromherz, M. T. Rispens, L. Sanchez, and J. C. Hummelen, Adv. Funct. Mater. **11**, 374 (2001).
[13] A. J. Nozik, Physica E (Amsterdam) **14**, 115 (2002).
[14] B. A. Gregg, in *Molecules as Components in Electronic Devices*, edited by M. Lieberman (American Chemical Society, Washington, D.C., 2002).
[15] I. H. Campbell, T. W. Hagler, D. L. Smith, and J. P. Ferraris, Phys. Rev. Lett. **76**, 1900 (1996).
[16] Z. D. Popovic, A.-M. Hor, and R. O. Loutfy, Chem. Phys. **127**, 451–457 (1988).
[17] S. J. Fonash, *Solar Cell Device Physics* (Academic, New York, 1981).
[18] B. A. Gregg, M. A. Fox, and A. J. Bard, J. Phys. Chem. **94**, 1586 (1990).
[19] B. A. Gregg, in *Semiconductor Photochemistry and Photophysics*; Vol. 10, edited by K. S. Schanze and V. Ramamurthy (Marcel Dekker, New York, 2002), pp. 51–87.
[20] B. A. Gregg, Appl. Phys. Lett. **67**, 1271 (1995).
[21] C. W. Tang, Appl. Phys. Lett. **48**, 183 (1986).
[22] B. A. Gregg, J. Sprague, and M. Peterson, J. Phys. Chem. B **101**, 5362 (1997).
[23] A. A. Zakhidov and K. Yoshino, Synth. Met. **64**, 155 (1994).
[24] V. M. Kenkre, P. E. Parris, and D. Schmidt, Phys. Rev. B **32**, 4946 (1985).
[25] Y. Wang and A. Suna, J. Phys. Chem. B **101**, 5627 (1997).
[26] B. A. Gregg, F. Pichot, S. Ferrere, and C. L. Fields, J. Phys. Chem. B **105**, 1422 (2001).
[27] J. E. Moser and M. Grätzel, Chem. Phys. **176**, 493 (1993).
[28] K. Kalyanasundaram and M. Grätzel, Coord. Chem. Rev. **77**, 347 (1998).
[29] S. A. Haque, Y. Tachibana, D. R. Klug, and J. R. Durrant, J. Phys. Chem. B **102**, 1745 (1998).
[30] J. S. Salafsky, W. H. Lubberhuizen, E. van Faassen, and R. E. I. Schropp, J. Phys. Chem. B **102**, 766 (1998).
[31] S. A. Haque, Y. Tachibana, R. L. Willis, J. E. Moser, M. Grätzel, D. R. Klug, and J. R. Durrant, J. Phys. Chem. B **104**, 538 (2000).
[32] F. Pichot and B. A. Gregg, J. Phys. Chem. B **104**, 6 (2000).
[33] B. A. Gregg and Y. I. Kim, J. Phys. Chem. **98**, 2412 (1994).

[34] G. G. Malliaras, J. R. Salem, P. J. Brock, and J. C. Scott, J. Appl. Phys. **84**, 1583 (1998).
[35] C. M. Ramsdale, J. A. Barker, A. C. Arias, J. D. MacKenzie, R. H. Friend, and N. C. Greenham, J. Appl. Phys. **92**, 4266 (2002).
[36] I. Prigogine, *Thermodynamics of Irreversible Processes*, 3rd ed. (Wiley, New York, 1967).
[37] W. J. Moore, *Physical Chemistry*, 4th ed. (Prentice-Hall, Engelwood Cliffs, New Jersey, 1972).
[38] R. J. D. Miller, G. L. McLendon, A. J. Nozik, W. Schmickler, and F. Willig, *Surface Electron Transfer Processes* (VCH, New York, 1995).
[39] J. Ferber and J. Luther, J. Phys. Chem. B **105**, 4895 (2001). Although the authors did not emphasize this result, see Figs. 9 and 10.
[40] D. Cahen, G. Hodes, M. Grätzel, J. F. Guillemoles, and I. Riess, J. Phys. Chem. B **104**, 2053 (2000).
[41] B. Kraabel, D. McBranch, N. S. Sariciftci, D. Moses, and A. J. Heeger, Phys. Rev. B **50**, 18 543 (1994).
[42] D. W. Winston, PhD Thesis, University of Colorado, 1996.
[43] H. Z. Fardi, D. W. Winston, R. E. Hayes, and M. C. Hanna, IEEE Trans. Electron Devices **47**, 915 (2000).
[44] B. A. Gregg and R. A. Cormier, J. Am. Chem. Soc. **123**, 7959–7960 (2001).
[45] G. Hodes, I. D. J. Howell, and L. M. Peter, J. Electrochem. Soc. **139**, 3136–3140 (1992).
[46] M. Pfeiffer, A. Beyer, T. Fritz, and K. Leo, Appl. Phys. Lett. **73**, 3202 (1998).
[47] See EPAPS Document No. E-JAPIAU-93-079306 for four pages of text on device and parameter files from our simulations. This document may be retrieved via the EPAPS homepage (http://www.aip.org/pubservs/epaps.html) or from ftp.aip.org in the directory/epaps/. See the EPAPS homepage for more information.